Fuel 211 (2018) 130–139

Contents lists available at ScienceDirect

Fuel

journal homepage: www.elsevier.com/locate/fuel

Full Length Article

Refractive index of biodiesel-diesel blends from effective polarizability and density

M. Colman[a], P.A. Sorichetti[b], S.D. Romano[c,*]

[a] Universidad de Buenos Aires, Facultad de Ingeniería, Grupo de Energías Renovables (GER), Av. Paseo Colón 850 (1063), Buenos Aires, Argentina
[b] Universidad de Buenos Aires, Facultad de Ingeniería, Laboratorio de Sistemas Líquidos, Av. Paseo Colón 850 (1063), Buenos Aires, Argentina
[c] Universidad de Buenos Aires, Consejo Nacional de Investigaciones Científicas y Técnicas, Instituto de Tecnologías del Hidrógeno y Energías Sostenibles (ITHES), Facultad de Ingeniería, Grupo de Energías Renovables (GER), Paseo Colón 850 (1063), Buenos Aires, Argentina

ARTICLE INFO

Keywords:
Refractive index
Biodiesel-diesel blends
Effective polarizability
Density

ABSTRACT

The refractive index of blends of soybean biodiesel with low sulfur diesel and also with ultra-low sulfur diesel was determined in the full composition range. Measurements were carried out acording to ASTM D1218/12 standard at 589 nm with an uncertainty of 2.10^{-4}. The temperature ranges were from 288 K to 328 K for blends with low sulfur diesel and from 293 K to 323 K for blends with ultra-low sulfur diesel.

The experimental results of refractive index as a function of temperature and composition were satisfactorily fitted to linear models with an uncertainty lower than 5.10^{-4} for blends with low sulfur diesel and 4.10^{-4} for ultra-low sulfur diesel blends.

The density of the blends was measured according to the ASTM D1298/12 standard in the same temperature range and the agreement with models available in the literature was satisfactorily checked. The effective polarizability of the blends was defined from the Lorentz-Lorenz equation using refractive index and density values. The effective polarizability for low sulfur diesel and ultra-low sulfur diesel were (0.3307 ± 0.0005) cm^3/g and (0.3327 ± 0.0005) cm^3/g respectively, and independent of temperature. These results are in good agreement with the published values for pure hydrocarbons and crude oils. For soybean biodiesel, a value of (0.3110 ± 0.0002) cm^3/g was obtained. It was also found that the effective polarizability of soybean biodiesel-diesel blends follows a linear dependence with composition. From our results, it also follows that the effective polarizability is independent of temperature, within the studied range.

From the values of effective polarizability of the pure fuels, together with the blend density at each temperature, it is then possible to estimate the refractive index of biodiesel-diesel blends in the full range of composition and studied temperatures, with an RMS difference below 6.10^{-4}.

1. Introduction

World energy consumption has increased in recent years due to motorization and industrialization processes, and fossil fuels are used by most countries to satisfy this growing demand. These energy resources are finite, non renewable, their reserves are found only in certain regions and their combustion releases large quantities of contaminants to the enviroment [1]. Diesel fuel is particularly important, since it is used for automotive and railway transport of industrial and agricultural goods.

Due to these concerns and in order to perserve the environment, it is urgent to search for alternative, economically viable and carbon-neutral fuels that can be obtained from a large variety of renewable sources. Biodiesel (BD) is an alternative fuel obtained from the transesterification of vegetable oils or animal fats [2]; it is non-toxic, biodegradable, with lower carbon dioxide and particulate emissions than fossil fuels [3]. BD is used in internal combustion engines, usually blended with diesel fuel. In many countries the use of biodiesel-diesel blends is regulated.

The characterization of líquid biofuels, fossil fuels and their blends is made according to international standards (ASTM D6751/15 [4], EN 14214/13 [5], etc.) where several properties are included, together with their acceptable ranges.

There are also alternative properties that are useful for biodiesel and blends characterization, such as permittivity, conductivity and speed of sound [6–8]. In the literature, dielectric properties at low frequencies

* Corresponding author at: Universidad de Buenos Aires. Consejo Nacional de Investigaciones Científicas y Técnicas. Instituto de Tecnologías del Hidrógeno y Energías Sostenibles (ITHES), Facultad de Ingeniería, Grupo de Energías Renovables (GER), Avenida Paseo Colón 850, Ciudad Autónoma de Buenos Aires (1063), Argentina.
E-mail addresses: sromano@fi.uba.ar, silviadromano@gmail.com (S.D. Romano).

http://dx.doi.org/10.1016/j.fuel.2017.09.050
Received 5 July 2017; Received in revised form 31 August 2017; Accepted 13 September 2017

were successful used to characterize feedstocks [9], biodiesel and its blends with diesel [10–12], and to detect contaminants [13]. However, measurements of dielectric properties at optical frequencies (i.e. refractive index) offer several advantages for characterization [14]. Particularly in the visible range, the technique is fast, accurate, simple, non destructive, and requires small sample volume. At present, there are several manufactures [15] that supply a wide variety of automatic refractometers, both for laboratory and inline control applications. Refractometry is widely used in many industries for concentration monitoring, dosage and quality control [15–16] including chemical, pharmaceutical, food/ beverage, sugar/bioethanol production, pulp, paper and textile, lubricant agents, and semiconductors, particulary for "inline" process control applications. In recent years [14], this technique has also been applied in biodiesel technology [17–23], for instance, to monitor the transesterification reaction [24–26], and to estimate the viscosity [27] and density of biodiesel-diesel blends [28]. The refractive index of biodiesel-diesel blends was studied for biodiesel of different origin: rapeseed biodiesel at temperatures between 298 and 323 K [23], for soybean biodiesel at 298 K [29] and Canola oil at 293 K [22].

As usual, in this work the volumetric percentage of the biofuel in the blend is indicated as Bx. For instance, B10 corresponds to 10% (v/v) biodiesel in the blend.

2. Materials and methods

2.1. Samples

The blends of soybean BD with diesel fossil fuel were prepared from two types of commercial diesel fossil fuel: low sulfur diesel (LSD) and ultra-low sulfur diesel (ULSD). The pure fuel samples were provided by a local refinery and complied with the ASTM D975/16 standard [30]. The same refinery provided the soybean biodiesel, according to ASTM D6751/15 specifications [4], that they use to prepare the commercial blend. Two series of samples were prepared: soybean BD-LSD blends in 5% steps, called Series 1, and soybean BD-ULSD blends in 10% steps called Series 2, in the full range of compositions (from B0 to B100).

2.2. Equipment

The refractive index of all samples was determined using an Abbe-type refractometer (Warkzawa Model RL-3) with an accuracy of 2.10^{-4}, according to the ASTM D1218/12 standard [31]. A 589 nm sodium arc lamp was used as a light source, and the sample cell temperature was kept constant within ± 0.1 K by a termostatic bath. The refractometer was calibrated using deionized water and toluene.

Density measurements of the samples were made with hydrometers according to ASTM D1298/12 standard [32] for the different density ranges, in a thermostatic bath, LAUDA, stabilized within ± 0.1 K. The measurement uncertainty was 10^{-3} g/cm^3.

2.3. Measurements

Refractive index measurements were made on both Series, according to the ASTM D1218/12 standard [31]. For Series 1, the temperature range was from 293 K to 328 K in 5 K steps, while for Series 2 the temperature range was from 298 K to 328 K, also in 5 K steps.

Density measurements were made in the temperature range between 303 K and 323 K in 5 K steps. The studied samples were LSD and ULSD pure diesel (B0), B30 and B70 from both series and pure biodiesel (B100). Measurements were carried out according to ASTM D1298/12 standard [32].

3. Theory

At optical frequencies, permittivity is generally controlled by

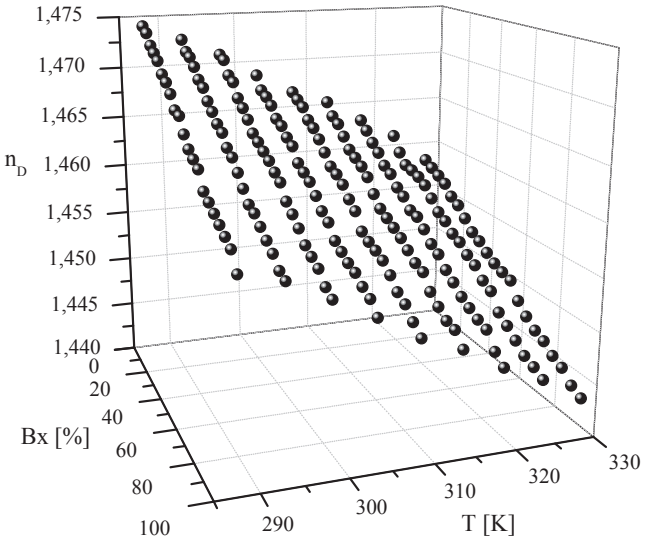

Fig. 1. Refractive index as a function of temperature and BD content (Series 1).

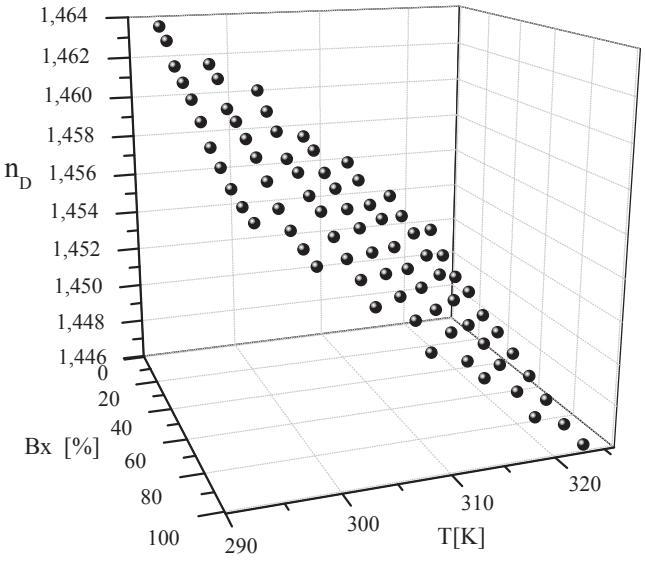

Fig. 2. Refractive index as a function of temperature and BD content (Series 2).

electronic polarization processes and refractive index measurements are commonly used to determine it [14]. In biodiesel, diesel fuel and their blends, the optical attenuation is small and the magnetic permittivity is practically equal to the vacuum value; therefore, the refractive index in the visible range can be written as:

$$n(\omega) = \sqrt{\varepsilon'(\omega)} \tag{1}$$

where $n(\omega)$ is the refractive index and $\varepsilon'(\omega)$ is the permittivity. Usually the refractive index is measured at the frequency, ω, corresponding to the sodium Na_D emission line (vacuum wavelength of 589 nm), indicated as n_D [14].

At optical frequencies, the Lorentz-Lorenz equation (Eq. (2)) is applied to estimate the polarizability, α, of pure substances as a function of refractive index, n, density, ρ, and molar mass, MW [33].

$$\alpha = \frac{n^2-1}{n^2+2} * \frac{MW}{\rho}\left(\frac{3}{4\pi N_A}\right) \tag{2}$$

where α is in cm^3, density in g/cm^3, molar mass in mol/g and N_A is the Avogadro constant, in mol^{-1}. Therefore, Eq. (2) may be written as:

$$\alpha = A*Rm \tag{3}$$

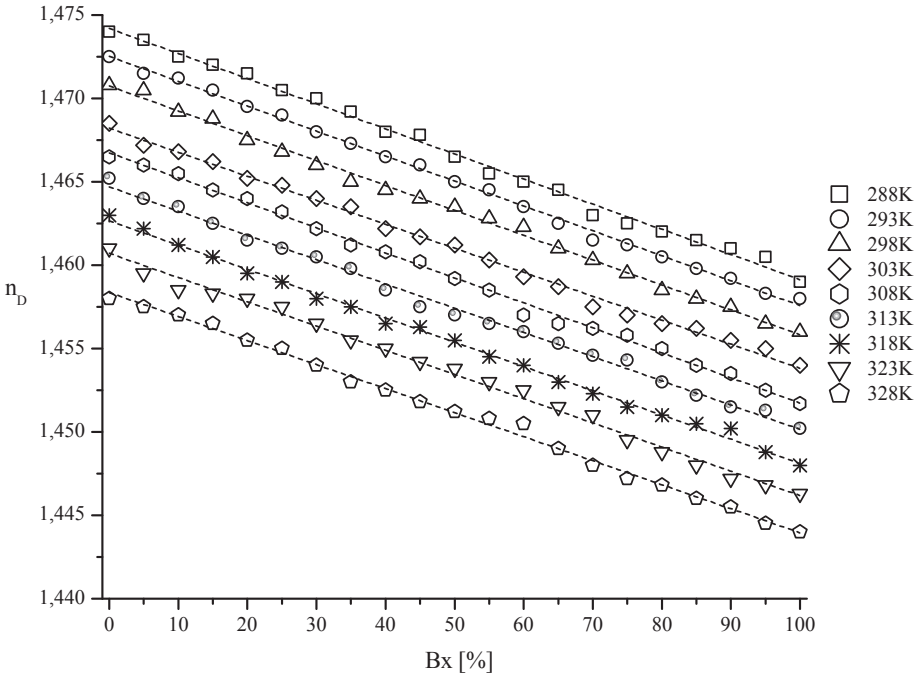

Fig. 3. Refractive index of Series 1 as a function of biodiesel content. The symbols indicate the experimental values at each temperature, and the lines correspond to the fitting to Eq. (5).

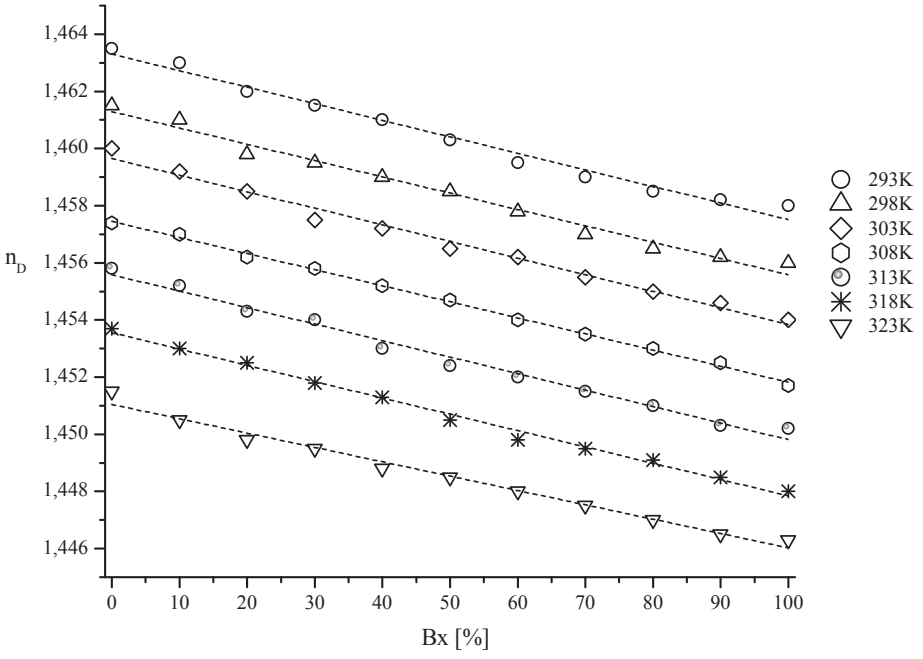

Fig. 4. Refractive index of Series 2 as a function of biodiesel content. The symbols indicate the experimental values at each temperature, and the lines correspond to the fitting to Eq. (5).

where A is a constant given by $\frac{3}{4\pi N_A}$ in mol and Rm is the molar refractivity, in cm^3/mol. To extend this definition to include mixtures of pure substances, we introduce the effective polarizability, $\bar{\alpha}$, given by:

$$\bar{\alpha} = \frac{n^2-1}{n^2+2} * \frac{1}{\rho} \quad (4)$$

where $\bar{\alpha}$ is in cm^3/g. It is interesting to mention that Bykov [34] in 1984 and then Vargas et al. [35–36] in 2009, experimentally found that the effective polarizability given by Eq. (4), for a wide variety of pure hydrocarbons and also for crude oils, is a constant practically equal to 1/3, and independent of temperature and pressure ("One-Third Rule").

4. Results and discussion

4.1. Refractive index

Figs. 1and 2 show the tridimensional plot of the experimental values of the refractive index as a function of temperature and composition, for Series 1 (biodiesel-LSD) and Series 2 (biodiesel-ULSD), respectively. It may be seen that both surfaces are smooth and regular.

In order to analyze the dependence of refractive index with biodiesel content, the surface *n(Bx,T)* can be projected onto the (*n,Bx)* plane. Figs. 3 and 4 show the projections for Series 1 and Series 2, respectively. The refractive index at each temperature decreases linearly with increasing biodiesel content in the blend.

The dashed lines in Figs. 3 and 4 correspond to the fitting of the

Table 1
Fitting parameters of Eq. (5) with their uncertainties for each temperature (Series 1 and Series 2).

Temperature [K]	dn_D/dBx $[\%^{-1}]$	$\Delta dn_D/dBx$ $[\%^{-1}]$	$n_D(Br,T)$	$\Delta n_D(Br,T)$	R^2	$\Delta n_D(Bx,T)$
Series 1						
288.1	−0.00015	< 0.000003	1.4667	< 0.00007	0.996	< 0.0004
293.1	−0.00015	< 0.000003	1.4650	< 0.00005	0.998	< 0.0003
298.1	−0.00015	< 0.000003	1.4633	< 0.00006	0.997	< 0.0003
303.1	−0.00014	< 0.000003	1.4610	< 0.00007	0.996	< 0.0003
308.1	−0.00015	< 0.000003	1.4592	< 0.00006	0.997	< 0.0003
313.1	−0.00015	< 0.000003	1.4574	< 0.00007	0.996	< 0.0004
318.1	−0.00015	< 0.000003	1.4554	< 0.00006	0.997	< 0.0003
323.1	−0.00015	< 0.000003	1.4534	< 0.00008	0.994	< 0.0004
328.1	−0.00014	< 0.000003	1.4512	< 0.00006	0.996	< 0.0003
Series 2						
293.1	−0.00006	< 0.000003	1.4604	< 0.00008	0.9839	< 0.0003
298.1	−0.00006	< 0.000003	1.4584	< 0.00008	0.9842	< 0.0003
303.1	−0.00006	< 0.000003	1.4567	< 0.00007	0.9880	< 0.0003
308.1	−0.00005	< 0.000001	1.4546	< 0.00003	0.9981	< 0.0001
313.1	−0.00006	< 0.000002	1.4527	< 0.00006	0.9911	< 0.0002
318.1	−0.00006	< 0.000002	1.4507	< 0.00005	0.9937	< 0.0002
323.1	−0.00005	< 0.000002	1.4480	< 0.00006	0.9897	< 0.0002

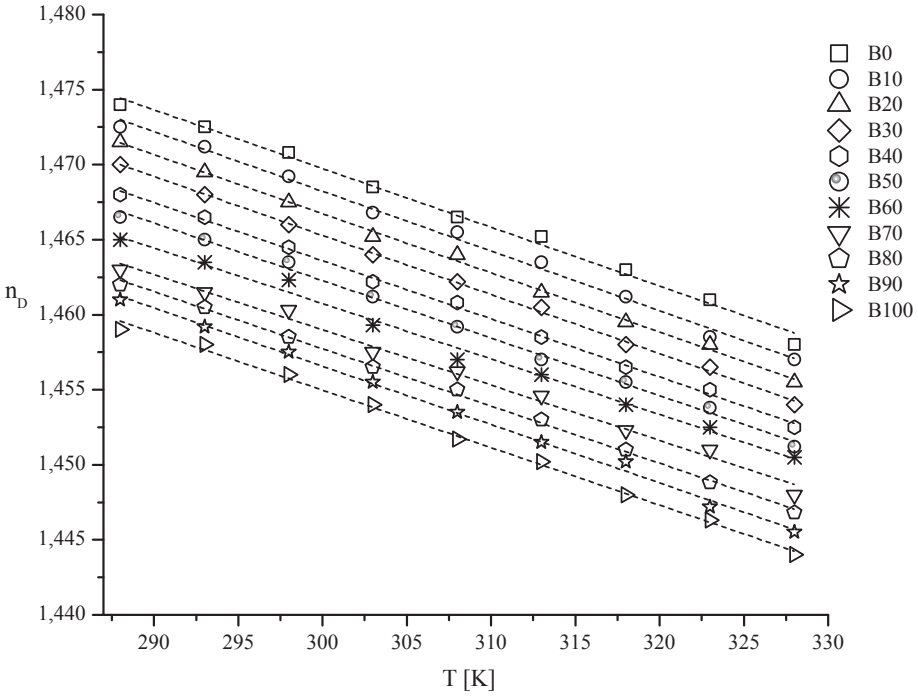

Fig. 5. Refractive index as a function of temperature. The symbols correspond to each composition and the dashed lines to the fitting of Eq. (6) (Series 1).

experimental data to a linear model at each temperature, according to Eq. (5):

$$n_D(Bx,T) = n_D(Br,T) + \left.\frac{dn_D}{dBx}\right|_T (Bx-Br) \quad (5)$$

where $n_D(Bx,T)$ is the refractive index as a function of composition, Bx, $n_D(Br,T)$ is the refractive index of the reference blend Br (50% biodiesel), and $\left.\frac{dn_D}{dBx}\right|_T$ is the slope, all measured at each temperature T.

The fitting parameters of Eq. (5), $\left.\frac{dn_D}{dBx}\right|_T$ and $n_D(Br,T)$, together with their uncertainties $\Delta\left.\frac{dn_D}{dBx}\right|_T$ and $\Delta n_D(Br,T)$, the determination coefficient R^2 and the RMS uncertainty $\Delta n_D(Bx,T)$ for Series 1 and Series 2 are shown in Table 1.

At all the measured temperatures, the refractive index of LSD is significantly different from ULSD. From Table 1 it can be seen that at each temperature, the refractive index decreases with increasing biodiesel content in the blend; the slope is higher for Series 1. Eq. (5) fits satisfactorily the experimental data of both series at all temperatures, with a determination coefficient higher than 0.983. The RMS uncertainty for both series was lower than 4.10^{-4}.

In order to analyze the dependence of refractive index on temperature, the surface $n_D(Bx,T)$ for both series may be projected onto the (n_D,T) plane. Figs. 5 and 6 show the experimental data (symbols) of refractive index for Series 1 and Series 2 respectively, as a function of temperature, for each composition. For the sake of clarity, in Fig. 5 only the compositions that correspond to 10% steps are shown. It can be seen that the refractive index of both series decreases linearly with increasing temperature at all the studied compositions.

Dashed lines in Figs. 5 and 6 correspond to the fitting of a linear model at each composition, according to Eq. (6).

$$n_D(Bx,T) = n_D(Bx,T_r) + \left.\frac{dn_D}{dT}\right|_{Bx} (T-T_r) \quad (6)$$

where $n_D(Bx,T)$ is the refractive index as a function of temperature, T,

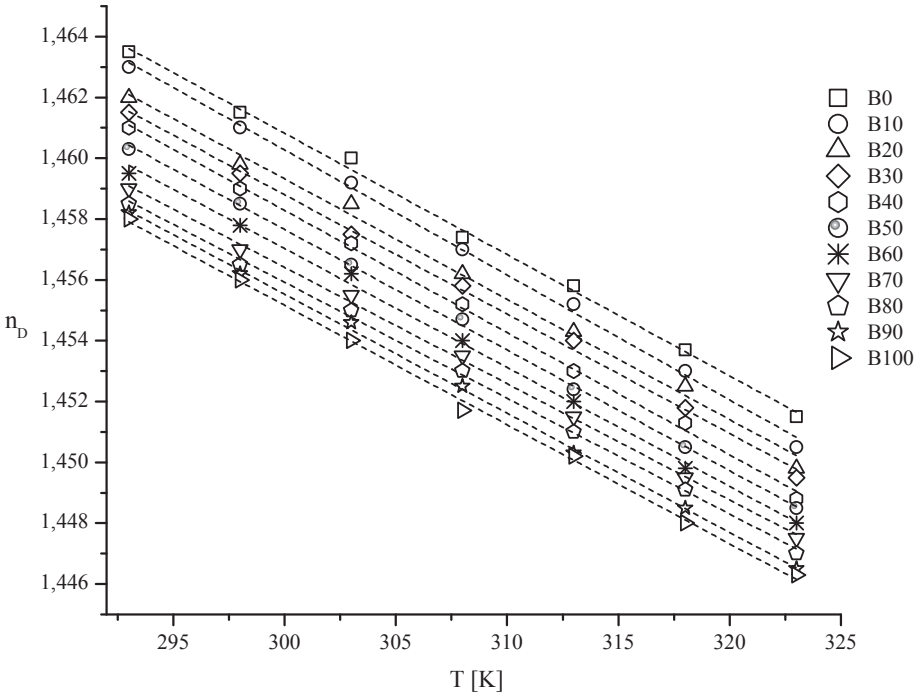

Fig. 6. Refractive index as a function of temperature. The symbols correspond to each composition and the dashed lines to the fitting of Eq. (6) (Series 2).

Table 2
Fitting parameters of Eq. (6) and their uncertainties for each composition (Series 1 and Series 2).

Sample	dn_D/dT $[K^{-1}]$	$\Delta dn_D/dT$ $[K^{-1}]$	$n_D(Bx,T_r)$	$\Delta n_D(Bx,T_r)$	R^2	$\Delta n_D(Bx,T)$
Series 1						
B0	−0.000391	< 0.000002	1.4647	< 0.0002	0.9941	< 0.0005
B5	−0.000399	< 0.000001	1.4638	< 0.0002	0.9940	< 0.0005
B10	−0.000398	< 0.000001	1.4631	< 0.0002	0.9952	< 0.0005
B15	−0.000396	< 0.000007	1.4624	< 0.0002	0.9983	< 0.0003
B20	−0.000394	< 0.000007	1.4616	< 0.0001	0.9979	< 0.0003
B25	−0.000386	< 0.000006	1.4610	< 0.0001	0.9985	< 0.0003
B30	−0.000393	< 0.000007	1.4602	< 0.0001	0.9987	< 0.0003
B35	−0.000396	< 0.000008	1.4594	< 0.0001	0.9977	< 0.0003
B40	−0.000387	< 0.000007	1.4586	< 0.0001	0.9981	< 0.0003
B45	−0.000397	< 0.000008	1.4580	< 0.0001	0.9977	< 0.0003
B50	−0.000383	< 0.000009	1.4573	< 0.0002	0.9969	< 0.0004
B55	−0.000379	< 0.000009	1.4566	< 0.0002	0.9963	< 0.0004
B60	−0.000370	< 0.000001	1.4559	< 0.0002	0.9925	< 0.0005
B65	−0.000381	< 0.000008	1.4550	< 0.0001	0.9975	< 0.0003
B70	−0.000368	< 0.000001	1.4542	< 0.0002	0.9925	< 0.0005
B75	−0.000383	< 0.000001	1.4535	< 0.0002	0.9926	< 0.0005
B80	−0.000381	< 0.000006	1.4528	< 0.0001	0.9983	< 0.0003
B85	−0.000388	< 0.000007	1.4521	< 0.0001	0.9982	< 0.0003
B90	−0.000389	< 0.000009	1.4515	< 0.0002	0.9969	< 0.0004
B95	−0.000392	< 0.000009	1.4507	< 0.0002	0.9970	< 0.0004
B100	−0.000383	< 0.000009	1.4500	< 0.0002	0.9968	< 0.0004
Series 2						
B0	−0.000399	< 0.000009	1.4556	< 0.0001	0.9976	< 0.0003
B10	−0.000411	< 0.000009	1.4549	< 0.0001	0.9979	< 0.0003
B20	−0.000396	< 0.000001	1.4542	< 0.0001	0.9952	< 0.0003
B30	−0.000392	< 0.000008	1.4537	< 0.0002	0.9980	< 0.0003
B40	−0.000401	< 0.000008	1.4531	< 0.0001	0.9985	< 0.0002
B50	−0.000396	< 0.000005	1.4525	< 0.0001	0.9993	< 0.0002
B60	−0.000391	< 0.000009	1.4519	< 0.0001	0.9978	< 0.0003
B70	−0.000382	< 0.000007	1.4514	< 0.0001	0.9987	< 0.0002
B80	−0.000381	< 0.000007	1.4510	< 0.0001	0.9987	< 0.0002
B90	−0.000391	< 0.000006	1.4504	< 0.0001	0.9990	< 0.0002
B100	−0.000386	< 0.000001	1.4499	< 0.0002	0.9932	< 0.0004

$n_D(Bx,T_r)$ is the refractive index at the reference temperature T_r (313 K), and $\frac{dn_D}{dT}\Big|_{Bx}$ is the slope, all measured at each composition Bx.

The Table 2 presents the fitting parameters of Eq. (6) for Series 1 and Series 2, $\frac{dn_D}{dT}\Big|_{Bx}$ and $n_D(Bx,T_r)$, together with their uncertainties $\Delta\frac{dn_D}{dT}\Big|_{Bx}$ and $\Delta n_D(Bx,T_r)$, the determination coefficient R^2 and the RMS uncertainty $\Delta n_D(Bx,T)$ for each composition.

From Table 2, it can be seen that the refractive index decreases with increasing temperature with a constant slope in the two series. Eq. (6)

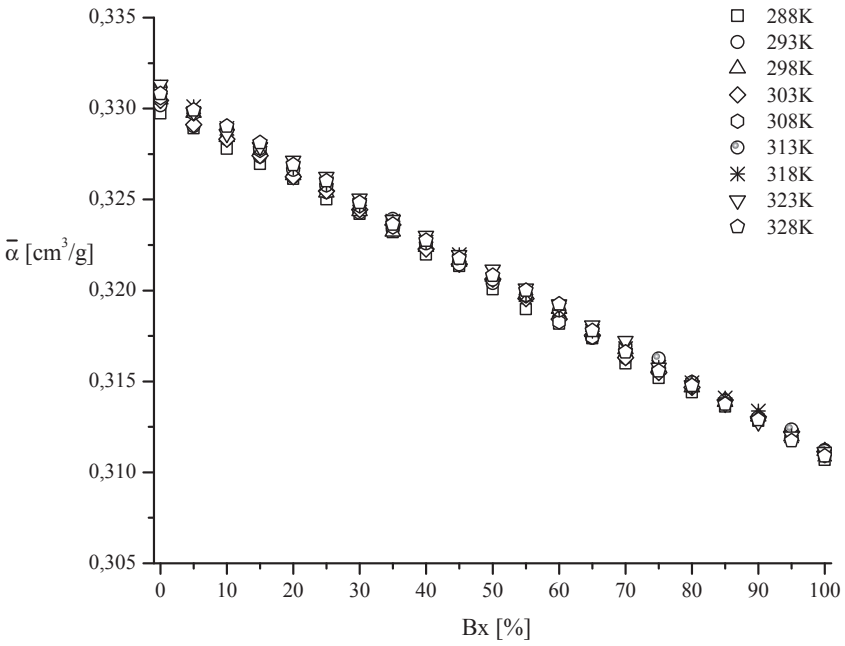

Fig. 7. Effective polarizability vs. biodiesel content. The symbols represent each temperature (Series 1).

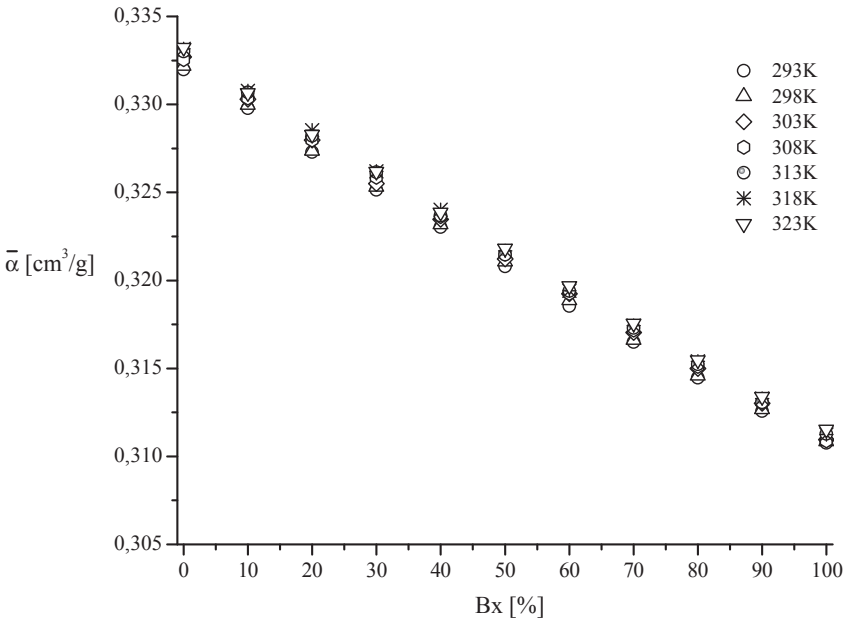

Fig. 8. Effective polarizability vs. biodiesel content. The symbols represent each temperature (Series 2).

fits satisfactorily to the experimental data, and the determination coefficient for all the studied samples was higher than 0.993. The RMS uncertainty was lower than 5.10^{-4} for both series. Furthermore, the refractive index of soybean biodiesel, LSD and ULSD at 298 K agree well with the values reported by Dunn [29].

4.2. Density

The dependence of density with temperature and composition of biodiesel-diesel blends is well known and several authors have proposed mathematical models that fit very satisfactorily to the experimental data [37–49]. In this work, it was found that our experimental data fit very well the empirical equation proposed by Yoon et al. [37] (Eq. (7)).

$$\rho(Bx,T) = a + bBx + cT + dTBx \quad (7)$$

In Eq. (7), $\rho(Bx,T)$ is the density in kg/m^3 as a function of temperature and composition, Bx is the biodiesel percentage in the sample in %, T is the temperature in °C and a, b, c and d are fitting parameters. Density measurements were carried out in Series 1 and Series 2, at temperatures between 303 K and 323 K.. In our samples, the coefficient d is statistically non-significant.

It is interesting to note that the substances studied by Yoon et al. correspond to the Series 2 in this work. The maximum RMS difference between our measured values and those calculated from Eq. (7) with Yoon's parameters is 0.002 g/cm^3.

4.3. Effective polarizability

According to Eq. (4), the effective polarizability of each sample, $\bar{\alpha}$, is calculated as the ratio between the refractive index factor, $(n^2 - 1/n^2 + 2)$, and the density, ρ. Since both the density and the low – frequency permittivity of biodiesel-diesel blends show an ideal behavior, it may be expected that the effective polarizability of these blends also

Table 3
Fitting parameters of Eq. (8) with their uncertainties for each temperature (Series 1 and Series 2).

Series 1						
Temperature	$d\bar{\alpha}/dBx$	$\Delta d\bar{\alpha}/dBx$	$\bar{\alpha}(Br,T)$	$\Delta\bar{\alpha}(Br,T)$	R^2	$\Delta\bar{\alpha}(Bx,T)$
[K]	*[cm³/g%]*	*[cm³/g%]*	*[cm³/g]*	*[cm³/g]*		*[cm³/g]*
288.1	−0.000191	< 0.0002	0.32021	< 0.00005	0.9989	< 0.0002
293.1	−0.000192	< 0.0002	0.32049	< 0.00004	0.9994	< 0.0002
298.1	−0.000194	< 0.0002	0.32068	< 0.00004	0.9991	< 0.0002
303.1	−0.000192	< 0.0002	0.32056	< 0.00005	0.9990	< 0.0002
308.1	−0.000198	< 0.0002	0.32074	< 0.00004	0.9992	< 0.0002
313.1	−0.000197	< 0.0002	0.3209	< 0.00005	0.9988	< 0.0003
318.1	−0.000199	< 0.0002	0.32091	< 0.00004	0.9992	< 0.0002
323.1	−0.000199	< 0.0002	0.32099	< 0.00005	0.9990	< 0.0003
328.1	−0.000202	< 0.0002	0.32086	< 0.00004	0.9993	< 0.0002
Series 2						
Temperature	$d\bar{\alpha}/dBx$	$\Delta d\bar{\alpha}/dBx$	$\bar{\alpha}(Br)$	$\Delta\bar{\alpha}(Br)$	R^2	$\Delta\bar{\alpha}(Bx)$
[K]	*[cm³/g%]*	*[cm³/g%]*	*[cm³/g]*	*[cm³/g]*		*[cm³/g]*
293.1	−0.000214	< 0.000003	0.33168	< 0.0002	0.9988	< 0.0003
298.1	−0.000214	< 0.000003	0.33187	< 0.0002	0.9989	< 0.0003
303.1	−0.000216	< 0.000003	0.33231	< 0.0002	0.9990	< 0.0003
308.1	−0.000216	< 0.000002	0.33239	< 0.0001	0.9997	< 0.0002
313.1	−0.000218	< 0.000003	0.33268	< 0.0002	0.9990	< 0.0003
318.1	−0.000219	< 0.000002	0.33287	< 0.0002	0.9993	< 0.0003
323.1	−0.000216	< 0.000003	0.33276	< 0.0002	0.9990	< 0.0003

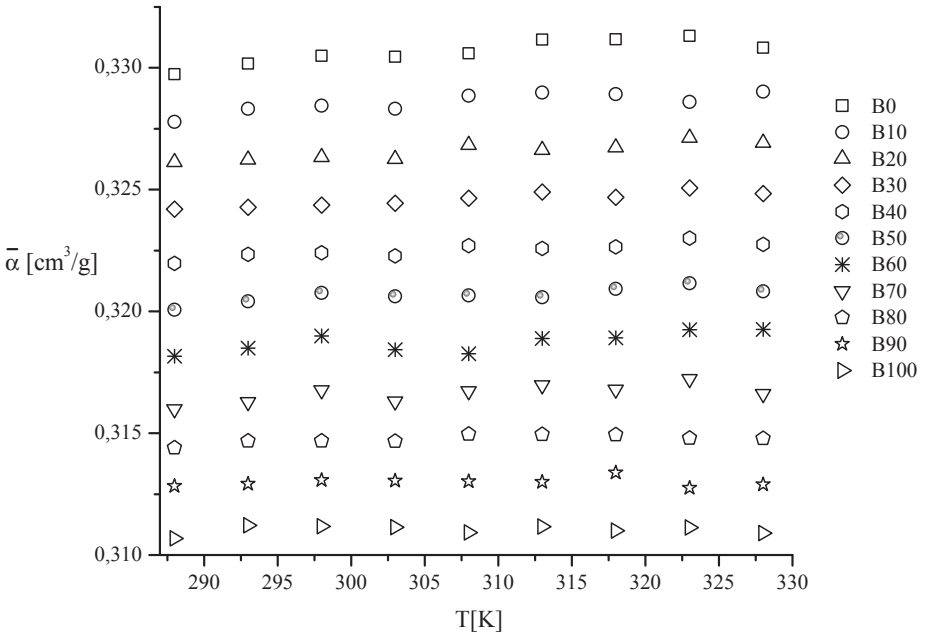

Fig. 9. Effective polarizability as a function of temperature for each sample (Series 1).

shows the same trend. This is reasonable given the similarities at the molecular level between diesel fossil fuel and biodiesel.

The effective polarizability as a function of biodiesel content for both series is shown in Figs. 7 and 8. It can be seen that, in fact, $\bar{\alpha}$ decreases linearly with increasing biodiesel content in the sample. The symbols represent the values at each temperature.

The calculated values of $\bar{\alpha}$ from both series were fitted to a linear model according to Eq. (8).

$$\bar{\alpha}(Bx,T) = \bar{\alpha}(Br,T) + \left.\frac{d\bar{\alpha}}{dBx}\right|_T (Bx-Br) \tag{8}$$

where $\bar{\alpha}(Bx,T)$ is the effective polarizability, in cm³/g, as a function of biodiesel content at temperature, T, in K, $\bar{\alpha}(Br,T)$ is the effective polarizability, in cm³/g, at the reference composition Br (50% of biodiesel), $\left.\frac{d\bar{\alpha}}{dBx}\right|_T$ is the slope, in $\%^{-1}$, and Bx is the biodiesel content in the sample, in %.

The fitting parameters of Eq. (8) for Series 1 and Series 2 are shown in Table 3, $\bar{\alpha}(Br,T)$ and $\left.\frac{d\bar{\alpha}}{dBx}\right|_T$, together with their uncertainties $\Delta\bar{\alpha}(Br,T)$ and $\Delta\left.\frac{d\bar{\alpha}}{dBx}\right|_T$, the determination coefficient R^2 and the RMS uncertainty of the estimation $\Delta\bar{\alpha}(Bx)$.

From Table 3 it may be seen that the determination coefficients are higher than those shown in Table 1 for the refractive index. In all cases they were higher than 0.9988.

The calculated values of $\bar{\alpha}$ as a function of temperature for both series are shown in Figs. 9 and 10 (symbols). For the sake of clarity, in Fig. 9 only the compositions that corresponds to 10% steps are shown.

From Figs. 9 and 10 it can be seen that the effective polarizability, in the studied range of temperatures, depends only on composition and it is independent of temperature. This is easy to see also in Figs. 7 and 8, since at each composition, the symbols corresponding to all the temperatures practically overlap. As a check, the average value of effective polarizability at each composition was calculated from the values at all the studied temperatures, together with its coefficient of variation. The results for Series 1 and Series 2 are given in Table 4.

The effective polarizability of LSD and ULSD, in the studied range of temperatures, is very close to 0.33, in good agreement with the "One-

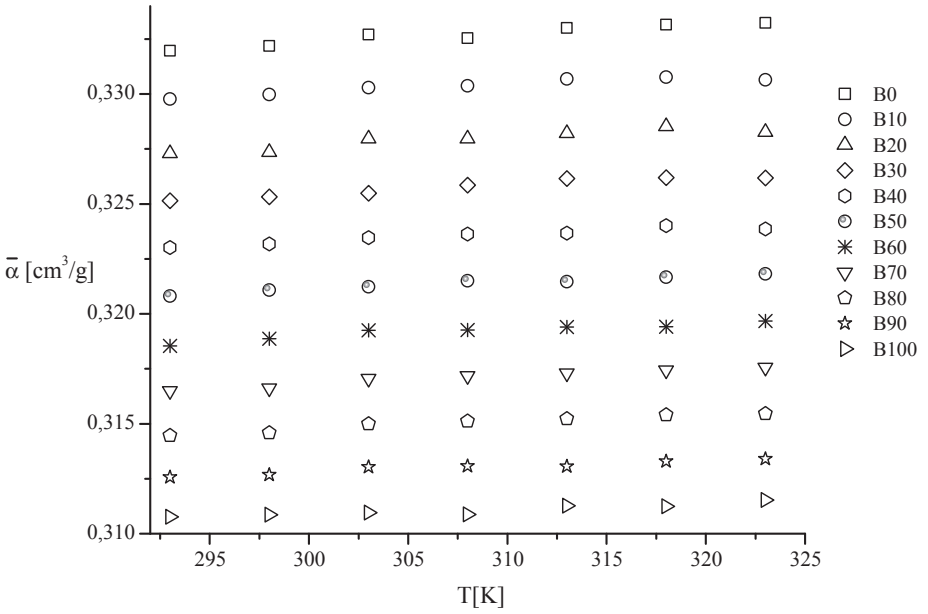

Fig. 10. Effective polarizability as a function of temperature for each sample (Series 2).

Table 4
Average values of $\bar{\alpha}$ for each composition (Series 1 and Series 2).

Sample	*Average $\bar{\alpha}$ [cm^3/g]*	*Coefficient of variation [%]*
Series 1		
B0	0.3307	0.16
B5	0.3296	0.13
B10	0.3286	0.12
B15	0.3276	0.11
B20	0.3266	0.11
B25	0.3257	0.12
B30	0.3246	0.09
B35	0.3236	0.08
B40	0.3225	0.09
B45	0.3216	0.07
B50	0.3207	0.10
B55	0.3197	0.10
B60	0.3187	0.13
B65	0.3177	0.08
B70	0.3166	0.12
B75	0.3157	0.10
B80	0.3148	0.06
B85	0.3138	0.05
B90	0.3130	0.06
B95	0.3120	0.06
B100	0.3110	0.06
Series 2		
B0	0.3327	0.14
B10	0.3304	0.11
B20	0.3279	0.14
B30	0.3258	0.14
B40	0.3236	0.11
B50	0.3214	0.11
B60	0.3192	0.12
B70	0.3171	0.13
B80	0.3150	0.12
B90	0.3130	0.10

Third rule" proposed by Bykov [34] and Vargas et al. [35,36] for crude oils and pure hydrocarbons.

For soybean biodiesel, the value of effective polarizability, in the studied range of temperatures, was (0.3110 ± 0.0002) cm^3/g. Effective polarizability values were also calculated, from published experimental data of refractive index and density, for biodiesel from sunflower [50], lard [50] and rapeseed [28] feedstocks. Interestingly, it was found that the average value of the effective polarizability of these substances was (0.310 ± 0.002) cm^3/g.

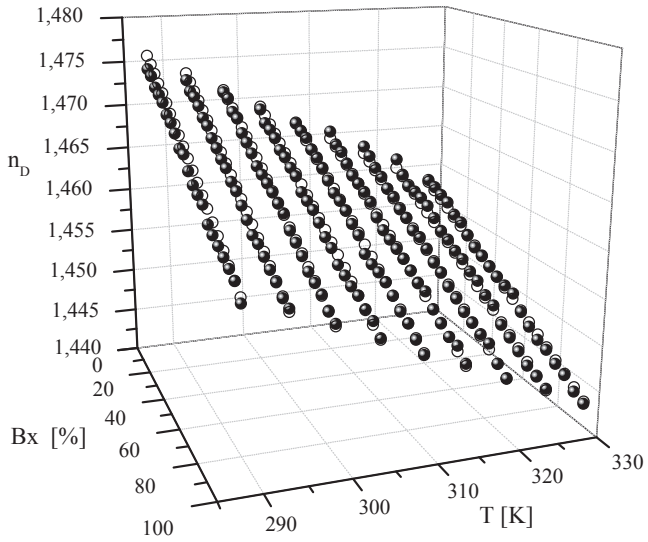

Fig. 11. Experimental (black symbols) and estimated (white symbols) values of refractive index as a function of temperature and composition for Series 1.

Given that the effective polarizability follows a linear dependence with biodiesel content and it is independent of temperature, its value for blends of any composition, in the studied range of temperature, can be easily estimated from the effective polarizability of the pure fuels (B0 and B100) (Eq. (9)).

$$\bar{\alpha}(Bx) = \bar{\alpha}(B0) - \frac{x}{100\%}[\bar{\alpha}(B0) - \bar{\alpha}(B100)] \quad (9)$$

where $\bar{\alpha}(Bx)$ is the effective polarizability of the blend of composition *Bx*, $\bar{\alpha}(B0)$ is the effective polarizability of diesel fossil fuel, $\bar{\alpha}(B100)$ is the effective polarizability of biodiesel, all in cm^3/g, and *x* is the biodiesel percentage in the sample, in %.

From the above, Eq. (9) was used to estimate the effective polarizability of each sample from Series 1 and Series 2 using the values of $\bar{\alpha}(B0)$ and $\bar{\alpha}(B100)$ from Table 4. The estimated values were compared with the effective polarizability calculated from the experimental values of refractive index (Fig. 3 and Fig. 4) and the density values from Eq. (7). The RMS difference for Series 1 and Series 2 was 3.10^{-4} cm^3/g and 5.10^{-4} cm^3/g, respectively.

The refractive index of each blend, as a function of temperature and

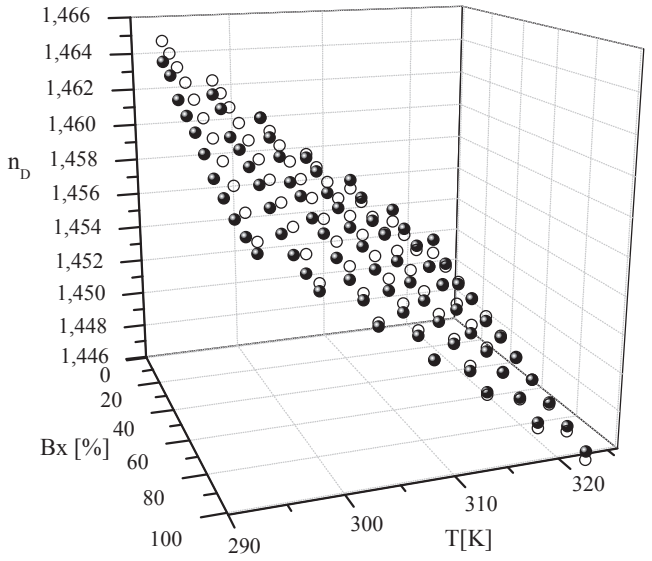

Fig. 12. Experimental (black symbols) and estimated (white symbols) values of refractive index as a function of temperature and composition for Series 2.

composition, was estimated using Eq. (4), from the effective polarizability of B0 and B100 (Eq. (9)) and the density given by Eq. (7). Figs. 11 and 12 show the experimental and estimated values of refractive index as a function of temperature and composition for both series. The RMS difference in both cases was lower than 6.10^{-4}.

5. Conclusion

The refractive index of blends of soybean biodiesel with diesel fuel (low sulfur and ultra-low sulfur) was measured according to ASTM D1218/12 standard, at 589 nm, with an uncertainty of 2.10^{-4}. The full range of composition was studied at a temperature range between 288 K and 328 K for low sulfur diesel blends and 293 K and 323 K for ultra-low sulfur diesel blends. It was verified that the refractive index can be fitted to a linear dependence both on temperature and composition. The determination coefficient was higher than 0.983 in all the studied samples.

The density of all samples was measured and the results were very satisfactorilt fitted by the model published by Yoon et al. The maximum RMS difference was 2.10^{-3}g/cm^{3,} at all temperatures and compositions. Using the refractive index and density values in the Lorentz-Lorenz equation, the effective polarizability is defined in this work for the pure fuels and for the biodiesel-diesel blends.

The effective polarizability for low sulfur and ultra-low sulfur diesel fossil fuels was found to be independent of temperature, with values of (0.3307 ± 0.0005) cm^3/g and (0.3327 ± 0.0005)cm^3/g respectively. This is in good agreement with the "One-Third rule" proposed by Bykov and Vargas for pure hydrocarbons and crude oils. The effective polarizability for biodiesel was also independent of temperature, with a value of (0.310 ± 0.002) cm^3/g. Interestingly, the effective polarizability of the biodiesel-diesel blends was found to be linearly depending on composition and independent of temperature, in the full studied range. The ideal behaviour of the effective polarizability with composition could be expected from the the dependence on composition of both density and permittivity at low frequencies, in diesel fossil fuel and biodiesel blends.

In conclusion, the effective polarizability of the blends can be calculated from the effective polarizability of the pure fuels. This makes possible, together with the density values of the samples, to estimate the refractive index of biodiesel-diesel blends. The difference between the the estimations and the experimental values of the refractive index was lower than 6.10^{-4} (RMS) in the full range of composition and at all the studied temperatures.

Acknowledgments

This work was supported by Projects UBACyT 20020120100062BA, 20020130100346BA, 20020160100084BA and 20020160100052BA, from the Universidad de Buenos Aires, Argentina (UBA). The authors thank Mr. Miguel Pellejero, Eng., (YPF Fuel Developing Laboratory) for the biodiesel and diesel fuel samples.

References

[1] Tang X, Höök M. Depletion of fossil fuels and anthropogenic climate change – a review. Energy Policy 2013;52:797–809.
[2] Romano SD, González Suárez E, Laborde MA. Combustibles alternativos. 2nd ed. Buenos Aires: Ediciones Cooperativas; 2006.
[3] Knothe G, Krahl J, Van Gerpen J. The biodiesel handbook. 2nd ed. Urbana: AOCS; Press; 2010.
[4] ASTM D6751-15ce1, Standard Specification for Biodiesel Fuel Blend Stock (B100) for Middle Distillate Fuels: ASTM International; 2015.
[5] UNE-EN 14214:2013 V2 + A1:2016 Liquid petroleum products - Fatty acid methyl esters (FAME) for use in diesel engines and heating applications - Requirements and test methods.
[6] Corach J, Sorichetti PA, Romano SD. Electrical and ultrasonic properties of vegetable oils and biodiesel. Fuel 2015;139:466–71.
[7] Corach J, Sorichetti PA, Romano SD. Electrical properties of mixtures of fatty acid methyl esters from different vegetable oils. Int J Hydrogen Energy 2012;37(19):14732–9.
[8] González Prieto LE, Sorichetti PA, Romano SD. Electric properties of biodiesel in the range from 20 Hz to 20 Mhz. Comparison with diesel fossil fuel. Int J Hydrogen Energy 2008;33(13):3531–7.
[9] Corach J, Sorichetti PA, Romano SD. Electrical properties of vegetable oils between 20 Hz and 2 MHz. Int J Hydrogen Energy 2014;39:8754–8.
[10] Corach J, Sorichetti PA, Romano SD. Permittivity of biodiesel-rich blends with fossil diesel fuel: application to biodiesel content estimation. Fuel 2016;177:268–73.
[11] Corach J, Sorichetti PA, Romano SD. Permittivity of diesel fossil fuel and blends with biodiesel in the full range from 0% to 100%: application to biodiesel content estimation. Fuel 2017;188:367–73.
[12] De Souza JE, Scherer MD, Cáceres JAS, Caires ARL, M'Peko JC. A close dielectric spectroscopic analysis of diesel/biodiesel blends and potential dielectric approaches for biodiesel content assessment. Fuel 2013;105:705–10.
[13] Romano SD, Sorichetti PA, Buesa Pueyo I. Methanol content in biodiesel estimated by flash point and electrical properties. In: Erbaum JB, editor. Bioethanol: production, benefits and economics. New York: NOVA Science Publishers Inc; 2009. p. 135–46.
[14] Romano SD, Sorichetti PA. Dielectric relaxation spectroscopy in biodiesel production and characterization. 1st ed. London: Springer Verlag; 2011.
[15] Liptak BG. Instrument engineers' handbook: process measurement and analysis, 4th ed. Vol. I, Chapter 8, section 8.52. CRC Press; 2003.
[16] Chianese A, Kramer HJ. Industrial crystallization process monitoring and control Ch. 8 Weinheim: Wiley-VCH Verlag & Co.; 2012.
[17] Check CJ, Bannister CD, Hawley JG, Davidson MG. Spectroscopic sensor techniques applicable to real-time biodiesel determination. Fuel 2010;89(2):457–61.
[18] Kawano MS, Kamikawachi RC, Fabris JL, Muller M. Thermally assisted sensor for conformity assessment of biodiesel production. Meas Sci Technol 2015;206.
[19] Possetti GRC, Côco LC, Yamamoto CI, de Arruda LVR, Falate R, Muller M, et al. Application of a long-period fibre grating-based transducer in the fuel industry. Meas Sci Technol 2009;20.
[20] Tubino M, Rocha JGJ, Favilla Bauerfeldt G. Biodiesel synthesis with alkaline catalysts: a new refractometric monitoring and kinetic study. Fuel 2014;125:164–72.
[21] Belle S, Scheurich S, Hellmann R, So S, Sparrow IJG, Emmerson GD. Refractive index sensing for online monitoring water and ethanol content in bio fuels. Proc. SPIE 7726, optical sensing and detection, 77261K (14 May 2010); doi:10.1117/12.853849; doi: 10.1117/12.853849.
[22] Kawano MS, Cardoso TKM, Possetti GRC, Kamikawachi RC, Fabris JL, Muller M. Sensing biodiesel and biodiesel-petrodiesel blends. OFS2012 22nd international conference on optical fiber sensors, 84215X (7 November 2012); doi:10.1117/12.945929.
[23] Geacai S, Nita I, Iulian O, Geacai E. Refractive index for biodiesel mixtures. U.P.B. Sci Bull (2012); Series B, Vol. 74, Iss. 4.
[24] Zabala S, Arzamendi G, Reyero I, Gandía LM. Monitoring of the methanolysis reaction for biodiesel production by off-line and on-line refractive index and speed of sound measurements. Fuel 2014;121:157–64.
[25] Santos RCR, Vieira RB, Valentini A. Monitoring the conversion of soybean oil to methyl or ethyl esters using the refractive index with correlation gas chromatography. Microchem J 2013;109:46–50.
[26] Ghanei R, Moradi GR, TaherpourKalantari R, Ajmandzadeh E. Variation of physical properties during transesterification of sunflower oil to biodiesel as an approach to predict reaction progress. Fuel Process Technol 2011;92:1593–8.
[27] Geacai S, Iulian O, Nita I. Measurement, correlation and prediction of biodiesel blends viscosity. Fuel 2015;143:268–74.
[28] Nita I, Geacai S, Iulian O. Measurements and correlation of physico-chemical

properties to composition of pseudo-binary mixtures with biodiesel. Renewable Energy 2011;36:3417–23.
[29] Dunn RO. Fuel properties of biodiesel/ultra-low sulfur diesel (ULSD) blends. J Am Oil Chemist's Soc 2011;88(12):1977–87.
[30] ASTM D975-16a, Standard specification for diesel fuel oils, West Conshohocken, PA: ASTM International; 2016.
[31] ASTM D1218-12(2016), Standard test method for refractive index and refractive dispersion of hydrocarbon liquids, West Conshohocken, PA: ASTM International; 2016.
[32] ASTM D1298-12b, Standard test method for density, relative density, or API gravity of crude petroleum and liquid petroleum products by hydrometer method, West Conshohocken, PA: ASTM International; 2012.
[33] Talebian E, Talebian M. A general review on the derivation of Clausius-Mossotti Relation. Optik 2013;124:2324–6.
[34] Bykov MI. Calculation of specific and molar refraction of hydrocarbons. Chem Technol Fuels Oils 1984;20:310–2.
[35] Vargas FM, Chapman WG. Application of the One-Third rule in hydrocarbon and crude oil systems. Fluid Phase Equilib 2010;290(1–2):103–8.
[36] Vargas FM, Gonzalez DL, Creek JF, Wang J, Buckley J, Hirasaki GJ, et al. Development of a general method for modeling asphaltene stability. Energy Fuels 2009;23:1147–54.
[37] Yoon SH, Park SH, Lee CS. Experimental investigation on the fuel properties of biodiesel and its blends at various temperatures. Energy Fuels 2008;22:652–6.
[38] Pratas MJ, Freitas S, Oliveira MB, Monteiro SC, Lima AS, Coutinho JAP. Biodiesel density: experimental measurements and prediction models. Energy Fuels 2011;25:2333–40.
[39] Alptekin E, Canakci M. Determination of the density and the viscosities of biodiesel-diesel fuel blends. Renewable Energy 2008;33:2623–30.
[40] Ramírez-Verduzco LF, García-Flores BE, Rodríguez-Rodríguez JE, del Rayo Jaramil-Jacob A. Prediction of the density and viscosity in biodiesel blends at various temperatures. Fuel 2011;90:1751–61.
[41] Tsanaktsidis C, Spinthiropoulos S, Tzilantonis G, Katsaros C. Variation of density of diesel and biodiesel mixtures in three different temperature ranges. Pet Sci Technol 2016;34(13):1121–8.
[42] Güllüm M, Bilgin A. Measurements and empirical correlations in predicting bio-diesel-diesel blends' viscosity and density. Fuel 2017;199:567–77.
[43] Güllüm M, Bilgin A. Density, flash point and heating value variations of corn oil biodiesel-diesel fuel blends. Fuel Process Technol 2015;134:456–64.
[44] Moradi GR, Karami B, Mohadesi M. Densities and kinematic viscosities in biodiesel-diesel blends at various temperatures. J Chem Eng Data 2013;58:99–105.
[45] Benjumea P, Agudelo J, Agudelo A. Basic properties of palm oil biodiesel–diesel blends. Fuel 2008;87:2069–75.
[46] Wakil MA, Kalam MA, Masjuki HH, Atabani AE, Rizwanul Fattah IM. Influence of biodiesel blending on physicochemical properties and importance of mathematical model for predicting the properties of biodiesel blend. Energy Convers Manage 2015;94:51–67.
[47] Rao GLN, Ramadhas AS, Nallusamy N, Sakthivel P. Relationships among the physical properties of biodiesel and engine fuel system design requirement. Int J Energy Environ 2010;1(5):919–26.
[48] Tat ME, Van Gerpen JH. The specific gravity of biodiesel and its blends with diesel fuel. J Am Oil Chemists' Soc 2000;77(2):115–9.
[49] Tesfa B, Mishra R, Gu F, Powles N. Prediction models for density and viscosity of biodiesel and their effects on fuel supply system in CI engines. Renewable Energy 2010;35(12):2752–60.
[50] Ivaniš GR, Radović IR, Veljković VB, Kijevčanin MLj. Biodiesel density and derived thermodynamic properties at high pressures and moderate temperatures. Fuel 2016;165:244–51.